

Tunable Kondo effect in double quantum dots coupled to ferromagnetic contacts

Rok Žitko,^{1,2} Jong Soo Lim,^{3,4} Rosa López,^{3,4} Jan Martinek,⁵ and Pascal Simon⁶

¹*Jožef Stefan Institute, Jamova 39, SI-1000 Ljubljana, Slovenia*

²*Faculty of Mathematics and Physics, University of Ljubljana, Jadranska 19, SI-1000 Ljubljana, Slovenia*

³*Departament de Física, Universitat de les Illes Balears, E-07122 Palma de Mallorca, Spain*

⁴*Institut de Física Interdisciplinària i de Sistemes Complexos IFISC (CSIC-UIB), E-07122 Palma de Mallorca, Spain*

⁵*Institute of Molecular Physics, Polish Academy of Sciences, Smoluchowskiego 17, 60-179 Poznań, Poland*

⁶*Laboratoire de Physique des Solides, CNRS UMR-8502, Univ. Paris Sud, 91405 Orsay Cedex, France*

(Dated: July 4, 2018)

We investigate the effects induced by spin polarization in the contacts attached to a serial double quantum dot. The polarization generates effective magnetic fields and suppresses the Kondo effect in each dot. The superexchange interaction (J_{AFM}), tuned by the inter-dot tunnelling rate t , can be used to compensate the effective fields and restore the Kondo resonance when the contact polarizations are aligned. As a consequence, the direction of the spin conductance can be controlled and even reversed using electrostatic gates alone. Furthermore, we study the associated two-impurity Kondo model and show that a ferromagnetic exchange coupling (J_{FM}) leads to an effective spin-1 exchange-anisotropic Kondo model which exhibits a quantum phase transition in the presence of partially polarized contacts.

PACS numbers: 72.10.Fk, 72.15.Qm

The study of spin-polarized transport in quantum dots (QDs), motivated by potential application for spintronic devices, has recently drawn a lot of attention both theoretically [1–4] and experimentally [5–7]. Ferromagnetic contacts affect the dot charge dynamics so that spin-dependent tunnelling rates renormalize differently the dot level for each spin orientation [1, 2, 4]. This is reflected in the appearance of an effective magnetic field in the dot [8–12] which suppresses the many-body Kondo state [11, 12], routinely observed at low enough temperatures in QDs. However, this Kondo state can be restored by properly tuning the QD level position (ϵ) via a gate potential [9, 10]. Additionally, when the polarizations in the ferromagnetic electrodes are non-collinear, the induced effective magnetic field depends on the relative orientation of the two easy-axis, but it can, again, be compensated [13].

Double quantum dots (DDs) have been extensively studied because they offer interesting perspectives in quantum spintronics such as spin-based quantum computation [14], Pauli spin blockade [15, 16], spin pumping [17], etc. Moreover, DDs offer a natural experimental realization of the two-impurity Kondo problem (2IKP) [18–20]. The interplay between the single dot Kondo effect and the interdot interaction has been extensively studied theoretically [21–24] and its experimental realization has been reported [25, 26]. Coupling such DDs to ferromagnetic contacts [27, 28] adds a further experimental handle to the system, which is distinct from applying an external magnetic field and may have interesting applications in spin-dependent transport.

In this letter we investigate the role of injecting spin-polarized charge carriers in serially coupled QDs (see upper inset in Fig. 1). We report pronounced transport phenomena due to the coupling with ferromagnetic electrodes, which are not present in single dots. In the absence of the particle-hole (p-h) symmetry, ferromagnetic contacts induce effective magnetic field in each QD. We show that for parallel magne-

tization in the electrodes, these induced effective fields can be compensated by properly tuning the inter-dot tunneling amplitude t , thereby restoring the Kondo states in each QD. Furthermore, we demonstrate the behaviour of the DD set-up as a controllable spin-filter device by gating the dots and varying either the lead polarization or, which is more useful, the inter-dot tunnelling t . Finally, we complete our study by analysing the role of the polarization on the 2IKP. In particular, we find that the equivalent model with a ferromagnetic spin-spin interaction J_{FM} behaves as a spin-1 exchange-anisotropic Kondo model and exhibits a Kosterlitz-Thouless quantum phase transition at finite polarization.

Model – The double dot set-up (Fig. 1) is modelled as a two-site Hubbard model. The Hamiltonian reads:

$$\mathcal{H} = \sum_{k,\sigma} \varepsilon_{\alpha k \sigma} c_{\alpha k \sigma}^\dagger c_{\alpha k \sigma} + \sum_{\sigma} \epsilon n_{\alpha \sigma} + U n_{\alpha \uparrow} n_{\alpha \downarrow} + t \sum_{\sigma} \left(d_{1\sigma}^\dagger d_{2\sigma} + \text{h.c.} \right) + \sum_{k,\sigma} \left(V_{\alpha} c_{\alpha k \sigma}^\dagger d_{\alpha \sigma} + \text{h.c.} \right), \quad (1)$$

Here $c_{\alpha k \sigma}$ annihilates an electron in the electrode $\alpha \in \{1, 2\}$ with wave-vector k and spin $\sigma = \uparrow, \downarrow$. Similarly, $d_{\alpha \sigma}$ destroys an electron with spin σ on the dot α . Each dot is also connected to a contact with hybridization amplitude V_{α} . Ferromagnetic contacts are described by employing spin-dependent tunnelling rates: $\Gamma_{\alpha, \sigma} = \pi |V_{\alpha}|^2 \nu_{\alpha \sigma}$, $\nu_{\alpha \sigma}$ being the spin-dependent density of states at in the contacts. The polarizations are parametrized by p_{α} , defined through $\Gamma_{\alpha, \uparrow} = \Gamma(1 + p_{\alpha})/2$, $\Gamma_{\alpha, \downarrow} = \Gamma(1 - p_{\alpha})/2$; we assume the total hybridization strength Γ to be constant and equal for both contacts. In this work we will consider the case of collinear polarization between the leads with parallel (P) ($p_1 = p_2 = p$) and anti-parallel (AP) alignment ($p_1 = -p_2 = p$). We solve \mathcal{H} using the numerical renormalization group technique (NRG) [29].

Particle-hole symmetric case, $\delta = \epsilon + U/2 = 0$. – The

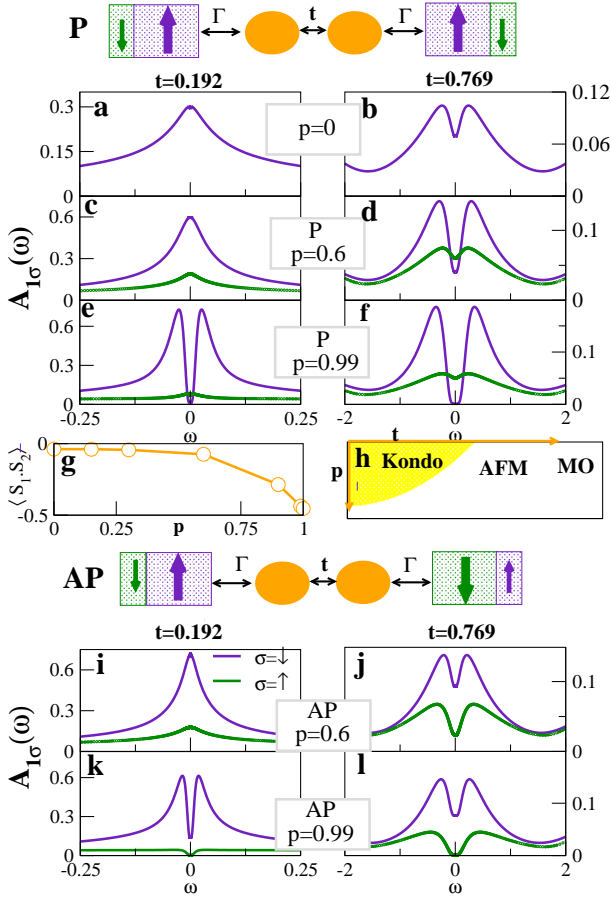


Figure 1. (Color online) Upper inset: Illustration of a serially coupled double dot set-up for the parallel P configuration [majority(minority) spins of both reservoirs are down(up) spins]. t is the inter-dot tunneling amplitude, Γ is the lead-dot hybridization strength. From (a) to (f): up and down spectral densities for the dot 1. Parameters are $\epsilon = -U/2$, $U = 7$, and $\Gamma = 1$. (g) Spin-spin correlation function for the P arrangement (1 and 2 sub-indices denote the left and right dot, respectively). (h) Double dot phase diagram for the P case when t and p are varied: the three phases are the Kondo phase, the anti-ferromagnetic phase (AFM) and the molecular-orbital phase (MO) in which for a very large t the two dots behave as an effective one-dot system with energy levels at $\epsilon \pm t$. In this case, the usual spin-1/2 Kondo physics emerges. Lower inset: Double dot system in the AP configuration [majority(minority) spins in the left reservoir are spin-up(down) electrons]. Up and down spectral densities for the dot 1 in the AP lead orientation are plotted in (i), (j), (k), and (l). Parameters are $\epsilon = -U/2$, $U = 7$, and $\Gamma = 1$.

dot-1 spectral functions $A_{1\sigma}(\omega)$ for the P and AP alignments are shown in Fig. 1. For $p = 0$ and small t [Fig. 1(a)], the spectral functions for both spin alignments show a single peak (the Kondo resonance) pinned at the Fermi level. As t increases, one moves from the regime dominated by the Kondo effect to a phase governed by the antiferromagnetic (AFM) coupling between the spins [Figs. 1(d), (e), and (f)]. The AFM regime is evidenced by a double-peak DOS with peaks at $\omega \approx \pm J/2$ where $J = J_{\text{AFM}} = 4t^2/U$ is the superex-

change interaction. For finite polarization, $p \neq 0$, each dot is predominantly affected by the polarization of the neighboring contact and only indirectly (thus weakly) by the other contact, therefore P and AP arrangements show similar behavior [cf. Fig. 1(a)-(f) and Fig. 1(i)-(l)]. For small t , in the P orientation, [Fig. 1(c)] the spectral weight at E_F becomes spin-dependent, i.e., $A_{1\uparrow}(E_F) \neq A_{1\downarrow}(E_F)$ but there is no spin-splitting. The width of the Kondo peak reduces according to [11] $T_K(p) \approx \tilde{D} \exp\{-1/(\nu_{\uparrow}J_K + \nu_{\downarrow}J_K)[\tanh^{-1}(p)/p]\}$ where $\nu J_K = 8\Gamma/\pi U$ at the p-h symmetry point. Thus, by increasing p [Fig. 1(e)], the Kondo temperature is lowered. When $J_{\text{AFM}} \gtrsim 2T_K(p)$, the Kondo effect is destroyed and the dot spins bind into a local singlet which is reflected in a split spectral density [Fig. 1(e)]. The correlation function ($S_1 \cdot S_2$) which measures the dot spins alignment is shown in Fig. 1(g) for increasing p for $t = -0.769$. Accordingly, the spectral function exhibits a splitting of magnitude J_{AFM} [Fig. 1(e)] signaling the formation of the AFM singlet state. This is the same type of cross-over that one observes in the $p = 0$ model as a function of t . This result implies that there is a continuous cross-over line in the (p, t) plane separating the Kondo phase from the AFM one. A schematic phase diagram summarizing this result is depicted in Fig. 1(h). Spectral dot densities in

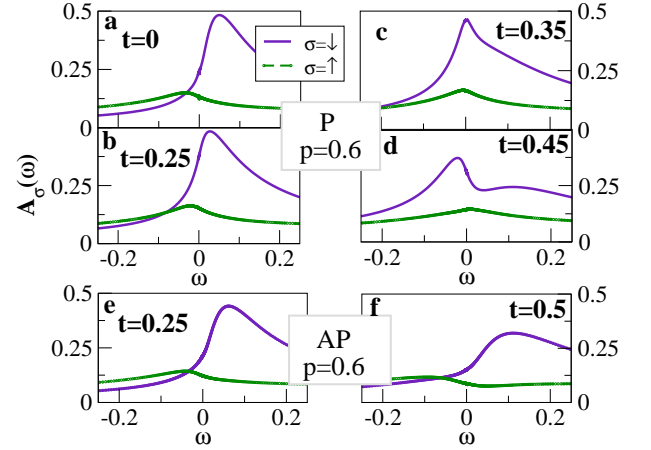


Figure 2. (Color online) Spectral function of dot 1 when the system is away from the particle-hole symmetric point. Parameters are $U = 7$, $\Gamma = 1$, $\epsilon = -U/2 + 1$.

the AP orientation are shown in Figs. 1(i)-(l). As mentioned previously, they exhibit a similar behaviour than in the P configuration. We find remarkable differences between the two magnetic orientations (P) and (AP) in the half-metallic limiting case when $p \rightarrow 1$ [illustrated in Fig. 1(e), and (f) for the P case and Fig. 1(k), and (l) for the AP case]. For the P case the spin-down spectral density at the Fermi level E_F ($\omega = 0$ in the plots) vanishes, while for AP it remains finite. Conversely, for the P arrangement the spin-up spectral function is finite at E_F , while for AP it goes to zero. The difference is due to an interference effect that can be studied analytically in the non-interacting ($U = 0$) limit, with the result holding more generally. For parallel alignment ($p \rightarrow 1$), spin-down

electrons are localized inside the DD system, while the spin-up electrons can still flow between the contacts; the $U = 0$ spectral function for spin-down electrons has delta-like peaks at $\omega = \pm t$ and is zero elsewhere, while the spin-up spectral function is finite at E_F . For AP, in the $p = 1$ limit the spin-up electrons from the contact 1 can enter both dots, but cannot exit at the right contact. The $U = 0$ spin-up spectral functions thus shows a peak at E_F for the dot 2 and, consequently, a null spectral density at E_F for the dot 1 due to interference. For the other electron spin, the behavior in the two dots is simply reversed. The difference in the $p \rightarrow 1$ limit becomes even more pronounced as t increases.

General case, $\delta \neq 0$. – Away from the p-h symmetric point, the spin splitting is generated by virtual processes proportional to the spin-dependent hybridization functions: $B_{\text{eff}} = \delta\epsilon_{\uparrow} - \delta\epsilon_{\downarrow}$ (with $\bar{\sigma} = -\sigma$)

$$\delta\epsilon_{\sigma} \approx -\frac{1}{\pi} \int d\omega \left\{ \frac{\Gamma_{\sigma}(\omega)[1 - f(\omega)]}{\omega - \epsilon} + \frac{\Gamma_{\bar{\sigma}}(\omega)f(\omega)}{\epsilon + U - \omega} \right\}. \quad (2)$$

Accordingly, at $p \neq 0$ and for general values of parameters, the spectral function exhibits spin splitting (see Fig. 2). For small t , this splitting is fully analogous to that observed in single QDs [e.g., see Fig. 2(a), and (b)]. For a single QD, in the AP case there is no induced field because of the direct compensation of the contributions from both contacts. In the DD case, however, there is an induced field in each dot for both P and AP cases, but they differ in the direction of the fields: they are aligned along the same direction for the P case ($B_{1,\text{eff}} = B_{2,\text{eff}}$), while they point in opposite directions for the AP case ($B_{1,\text{eff}} = -B_{2,\text{eff}}$). In single QDs, the splitting can only be restored by the application of an external magnetic field. In DDs, we find, in contrast, that the splitting compensation can also be achieved by the exchange fields due to the inter-dot exchange coupling J_{AFM} : for a specific value of t the compensation occurs [Fig. 2(c)] and beyond this t value the splitting is shown again [Fig. 2(d)]. This can be understood as follows: seen from dot 1(2), the exchange coupling J_{AFM} between the dots can be regarded as an effective magnetic field: $B_{\text{exc}} = J_{\text{AFM}}S_{z2(1)}$. The restoration is, however, only possible in the P case while in the AP case the splitting only grows when t is increased [see Fig. 2(e) and (f)]. Note that this type of restoration of the Kondo peak has also been predicted in the two-impurity Kondo problem in an external magnetic field [30, 31] and verified experimentally [32]. Interestingly, all these features shown in the dot spectral density are reflected in a measurable transport magnitude: the linear conductance. We compute the conductance through the DD system as a function of the inter-dot tunnelling t and the dot level position ϵ for three values of p in Fig. 3 (upper panel). For $p = 0$ we observe the standard results for the conductance of a DD: along the particle-hole symmetric line the conductance is low in the small- t and large- t limits, and it peaks at the cross-over point $J_{\text{AFM}} \sim 2T_K$. For very large t , the conductance becomes high when one of the molecular orbitals at energies $\epsilon \pm t$ is tuned to the Fermi level signaling the molecular orbital phase. The cross-over conductance peak

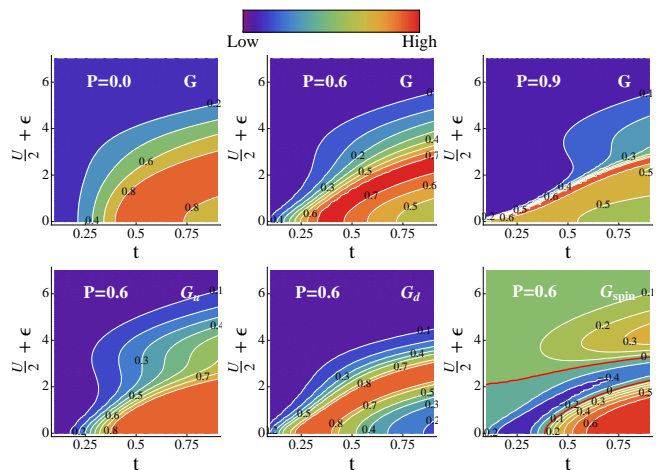


Figure 3. (Color online) Conductance plots versus $\delta = \epsilon + U/2$ and t . Upper panel: Linear conductance for $p = 0, 0.6, 0.9$ in the parallel arrangement. Lower panel: spin-up (left), spin-down (center) conductance and spin conductance (right) for $p = 0.6$. Parameters are $U = 7, \Gamma = 1$.

and the molecular-orbital conductance peak are smoothly connected in the (t, ϵ) plane by a high-conductance ridge which reaches the *unitary conductance*, $G = 2e^2/h$. The influence of polarized contacts is more dramatic for the P alignment, due to the interplay between J_{AFM} and the effective fields. The DD can namely behave as a *spin-filter* device for a finite polarization in the P arrangement. This can be seen from the spin-up conductance G_{\uparrow} , the spin-down conductance G_{\downarrow} , and the spin conductance $G_s = G_{\uparrow} - G_{\downarrow}$, which are shown in the lower panel of Fig. 3. For finite p the conductance ridge no longer reaches the unitary limit. The maximum conductance coincides with the restoration of the Kondo effect when $B_{\text{exc}} + B_{\text{eff}} = 0$. G_{\downarrow} exhibits a sharp peak in the (t, ϵ) plane; the narrow width is due to the weak hybridisation of the spin-down electrons that reduces the Kondo scale as p increases. As a consequence, one finds that *the direction and amplitude of the spin conductance G_s can be tuned by the parameters ϵ and t* (shown in Fig. 3). Therefore the DD acts as an efficient spin-filter device with potential applications in the construction of spintronic devices.

Equivalent two-impurity Kondo model. – We also study the associated Kondo model with direct inter-dot magnetic exchange coupling of the form $\mathcal{H} = JS_1 \cdot S_2$ and no hopping term, i.e., the hopping term t is replaced by a pure exchange term with $J = J_{\text{AFM}} = 4t^2/U$. Provided that the charge transfer term between the leads (which corresponds to a co-tunneling term through the two dots) can be neglected, one finds a true quantum phase transition which corresponds to the critical behavior in the 2IKM [24]. We found that polarization in the leads does not affect this conclusion. However, in an experimentally realistic system, this phase transition is replaced by a smooth cross-over as a function of t [33].

For completeness, we have also analysed the case of a ferromagnetic exchange interaction, i.e., $J = -J_{\text{FM}} < 0$. The cor-

responding spectral functions are shown in Fig. 4. For normal electrodes and small J_{FM} , each dot exhibits a single-channel spin-1/2 Kondo state, while for a large J_{FM} , the dot spins first rigidly bind at some high temperature into a spin-1 state which is then screened at a lower temperature. Note that the shape of the Kondo resonance is therefore different for small and large- J_{FM} cases [corresponding to Fig. 4(a) and Fig. 4(b), respectively]. At finite p [Fig. 4(c), and Fig. 4(f)], the Kondo effect is destroyed and the NRG results show that the DD setup has a residual $\ln 2$ entropy, indicating the occurrence of a quantum phase transition from the Kondo screened phase to a partially-screened phase. The transition is of the Kosterlitz-Thouless type and it occurs at a value of p which depends on J_{FM} . Thus, there is a line of phase transitions in the (p, J_{FM}) parameter plane. This behavior is not unexpected. It should be recalled that for a single QD, the presence of spin polarization results in the exchange-anisotropy of the effective low-energy Kondo model, $J_{\perp} \neq J_z$. The same effect is expected in the present spin-1 Kondo model. It is known, however, that anisotropic high-spin Kondo model feature partially-screened states in their phase diagrams [34].

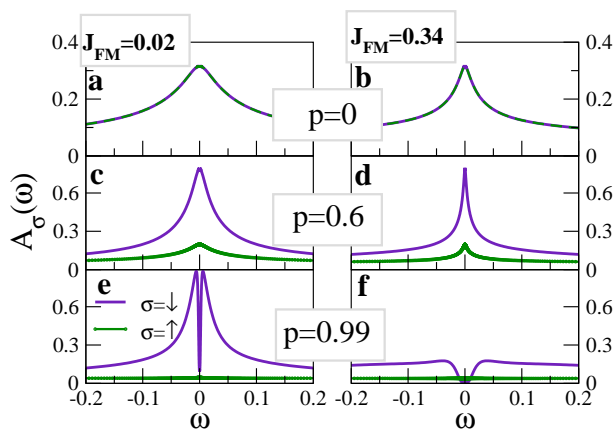


Figure 4. (Color online) Spectral functions for the model with ferromagnetic exchange coupling for three different polarizations $p = 0$, $p = 0.6$ and $p = 0.9$ (P case) and two distinct J_{FM} strength couplings.

Conclusion. – Ferromagnetic contacts alter profoundly the transport properties of serially coupled double dots. The interplay between the anti-ferromagnetic exchange coupling and the effective fields induced by the polarized leads in the parallel contact configuration may reinforce the Kondo effect. By tuning the interdot tunnelling and the dot gates the spin conductance reverses its sign, thus the DD acts as a spin-filter device. We have also shown that the 2IKM with ferromagnetic interaction exhibits a Kosterlitz-Thouless type transition ascribed to the partially spin polarized contacts. We propose double dot carbon nanotubes attached to polarized contacts as the best candidate to observe our predictions. In carbon nanotube quantum dots, large polarizations and much stronger Kondo states have been observed in comparison with semiconductor quantum dots [35–38]

RZ acknowledges the support of the Slovenian Research Agency (ARRS) under Grant No. Z1-2058. J.S and R.L. are supported by Spanish MICINN (Grant No. FIS2008-00781) and the Conselleria dInnovacio, Interior i Justicia Govern de les Illes Balears.

-
- [1] F. M. Souza, J. C. Egues, and A. P. Jauho, Phys. Rev. B **75**, 165303 (2007).
 - [2] P. Zhang, Q.-K. Xue, Y. Wang, and X. C. Xie, Phys. Rev. Lett. **89**, 286803 (2002).
 - [3] Y. Utsumi, J. Martinek, G. Schön, H. Imamura, and S. Maekawa, Phys. Rev. B **71**, 245116 (2005).
 - [4] K. Hamaya, M. Kitabatake, K. Shibata, M. Jung, S. Ishida, T. Taniyama, K. Hirakawa, Y. Arakawa, and T. Machida, Phys. Rev. Lett. **102**, 236806 (2009).
 - [5] A. N. Pasupathy, R. C. Bialczak, J. Martinek, J. E. Grose, L. A. K. Donev, P. L. McEuen, and D. C. Ralph, Science **306**, 86 (2004).
 - [6] M. R. Calvo, J. Fernandez-Rossier, J. J. Palacios, D. Jacob, D. Natelson, and C. Untiedt, Nature **104**, 036804 (2010).
 - [7] T. Kobayashi, S. Tsuruta, S. Sasaki, T. Fujisawa, Y. Tokura, and T. Akazaki, Phys. Rev. Lett. **104**, 036804 (2010).
 - [8] M. Sindel, L. Borda, J. Martinek, R. Bulla, J. König, G. Schön, S. Maekawa, and J. von Delft, Phys. Rev. B **76**, 045321 (2007).
 - [9] M.-S. Choi, D. Sánchez, and R. López, Phys. Rev. Lett. **92**, 056601 (2004).
 - [10] J. Martinek, M. Sindel, L. Borda, J. Barnas, R. Bulla, J. König, G. Schön, S. Maekawa, and J. von Delft, Phys. Rev. B **72**, 121302 (2005).
 - [11] J. Martinek, M. Sindel, L. Borda, J. Barna, J. König, G. Schön, and J. von Delft, Phys. Rev. Lett. **91**, 247202 (2003).
 - [12] J. Martinek, Y. Utsumi, H. Imamura, J. Barnas, S. Maekawa, J. König, and G. Schön, Phys. Rev. Lett. **91**, 127203 (2003).
 - [13] P. Simon, P. S. Cornaglia, D. Feinberg, and C. A. Balseiro, Phys. Rev. B **75**, 045310 (2007).
 - [14] D. Loss and D. DiVincenzo, Phys. Rev. A **57**, 120 (1998).
 - [15] K. Ono, D. G. Austing, Y. Tokura, and S. Tarucha, Science **297**, 1313 (2002).
 - [16] J. Fransson, Nanotechnology **17**, 5344 (2006).
 - [17] E. Cota, R. Aguado, and G. Platero, Phys. Rev. Lett. **94**, 107202 (2005).
 - [18] B. A. Jones and C. M. Varma, Phys. Rev. B **40**, 324 (1989).
 - [19] B. A. Jones, B. G. Kotliar, and A. J. Millis, Phys. Rev. B **39**, 3415 (1989).
 - [20] I. Affleck and A. W. W. Ludwig, Phys. Rev. Lett. **68**, 1046 (1992).
 - [21] A. Georges and Y. Meir, Phys. Rev. Lett. **82**, 3508 (1999).
 - [22] T. Aono and M. Eto, Phys. Rev. B **63**, 125327 (2001).
 - [23] G. Zaránd, C.-H. Chung, P. Simon, and M. Vojta, Phys. Rev. Lett. **97**, 166802 (2006).
 - [24] E. Sela and I. Affleck, Phys. Rev. Lett. **102**, 047201 (2009).
 - [25] H. Jeong, A. M. Chang, and M. R. Melloch, Science **293**, 2221 (2001).
 - [26] J. C. Chen, A. M. Chang, and M. R. Melloch, Phys. Rev. Lett. **92**, 176801 (2004).
 - [27] Y. Tanaka and N. Kawakami, J. Phys. Soc. Jpn **73**, 2795 (2004).
 - [28] R. Hornberger, S. Koller, G. Begemann, A. Donarini, and M. Grifoni, Phys. Rev. B **77**, 245313 (2008).
 - [29] K. Wilson, Rev. Mod. Phys. **47**, 773 (1975).
 - [30] P. Simon, R. Lopez, and Y. Oreg, Phys. Rev. Lett. **94**, 086602

- (2005).
- [31] M. G. Vavilov and L. I. Glazman, Phys. Rev. Lett. **94**, 086805 (2005).
- [32] H. B. Heersche, Z. de Groot, J. A. Folk, L. P. Kouwenhoven, H. S. J. van der Zant, A. A. Houck, J. Labaziewicz, and I. L. Chuang, Phys. Rev. Lett. **96**, 017205 (2006).
- [33] F. W. Jayatilaka, M. R. Galpin, and D. E. Logan, cond-mat:1106.5450 (2011).
- [34] A. Schiller and L. De Leo, Phys. Rev. B **77**, 075114 (2008).
- [35] H. T. Man, I. J. W. Wever, and A. F. Morpurgo, Phys. Rev. B **73**, 241401 (2006).
- [36] A. Cottet, T. Kontos, S. Sahoo, H. T. Man, M.-S. Choi, W. Belzig, C. Bruder, A. F. Morpurgo, and C. Schenberger, Semiconductor Science and Technology **21**, S78 (2006).
- [37] J. Hauptmann, J. Paaske, and P. Lindelof, Nat. Phys. **4**, 373 (2008).
- [38] C. Schenke, S. Koller, L. Mayrhofer, and M. Grifoni, Phys. Rev. B **80**, 035412 (2009).

Tunable Kondo effect in double quantum dot coupled to ferromagnetic contacts

Rok Žitko,^{1,2} Jong Soo Lim,³ Rosa López,^{3,4} Jan Martinek,⁵ and Pascal Simon⁶

¹*Jožef Stefan Institute, Jamova 39, SI-1000 Ljubljana, Slovenia*

²*Faculty of Mathematics and Physics, University of Ljubljana, Jadranska 19, SI-1000 Ljubljana, Slovenia*

³*Departament de Física, Universitat de les Illes Balears, E-07122 Palma de Mallorca, Spain*

⁴*Institut de Física Interdisciplinar i de Sistemes Complexos IFISC (CSIC-UIB), E-07122 Palma de Mallorca, Spain*

⁵*Institute of Molecular Physics, Polish Academy of Sciences, Smoluchowskiego 17, 60-179 Poznań, Poland*

⁶*Laboratoire de Physique des Solides, CNRS UMR-8502, Univ. Paris Sud, 91405 Orsay Cedex, France*

I. EQUATION OF MOTION STUDY OF THE NON-INTERACTING CASE, $U = 0$

We consider the $U = 0$ limit of the Hamiltonian presented in the main text. Our goal is to compute the spectral functions using the equation-of-motion method:

$$z\langle\langle A; B \rangle\rangle_z = \langle[A, B]_+\rangle + \langle\langle[A, H]_-; B \rangle\rangle_z \quad (1)$$

where z is the frequency parameter in the complex plane, $\langle\langle A; B \rangle\rangle_z$ denotes the correlator between the operators A and B , while $[A, B]_-$ and $[A, B]_+$ are a commutator and an anticommutator, respectively. We introduce the notation $G_{i\sigma, j\tau}(z) = \langle\langle d_{i\sigma}; d_{j\tau}^\dagger \rangle\rangle_z$ for the impurity Green's functions, where $i, j \in \{1, 2\}$ and $\sigma, \tau \in \{\uparrow, \downarrow\}$. Since the spin components along the z -axis are conserved, only $\sigma = \tau$ parts of the Green's function are non-zero, thus we may also write $G_{ij, \sigma}(z) \equiv G_{i\sigma, j\sigma}(z)$. Furthermore, we define $G_{\alpha k i, \sigma}(z) = \langle\langle c_{\alpha k \sigma}; d_{i\sigma}^\dagger \rangle\rangle_z$ where k is a wave-vector in the lead $\alpha \in \{1, 2\}$.

We obtain (omitting the argument z of Green's functions for brevity)

$$\begin{aligned} zG_{11, \sigma} &= 1 + \epsilon G_{11, \sigma} + tG_{21, \sigma} + V_1 \sum_k G_{1k1, \sigma}, \\ zG_{12, \sigma} &= \epsilon G_{12, \sigma} + tG_{22, \sigma} + V_1 \sum_k G_{1k2, \sigma}, \\ zG_{21, \sigma} &= \epsilon G_{21, \sigma} + tG_{11, \sigma} + V_2 \sum_k G_{2k1, \sigma}, \\ zG_{22, \sigma} &= 1 + \epsilon G_{22, \sigma} + tG_{12, \sigma} + V_2 \sum_k G_{2k2, \sigma}, \end{aligned} \quad (2)$$

and

$$zG_{\alpha k i, \sigma} = \epsilon_{\alpha k \sigma} G_{\alpha k i, \sigma} + V_\alpha G_{\alpha i, \sigma}. \quad (3)$$

From the latter equation it follows

$$G_{\alpha k i, \sigma} = \frac{V_\alpha}{z - \epsilon_{\alpha k \sigma}} G_{\alpha i, \sigma}. \quad (4)$$

We introduce the (spin-dependent) hybridization function as

$$\Delta_{\alpha\sigma} = \sum_k \frac{V_\alpha^2}{z - \epsilon_{\alpha k \sigma}}. \quad (5)$$

The spin dependence arises from the σ -dependence of the band dispersion $\epsilon_{\alpha k \sigma}$, i.e., from the spin dependence of the conduction-band density of states.

Solving the system of equation we obtain

$$\begin{aligned} G_{11, \sigma}(z) &= \frac{1}{z - \epsilon - \Delta_{1\sigma} - \frac{t^2}{z - \epsilon - \Delta_{2\sigma}}}, \\ G_{22, \sigma}(z) &= \frac{1}{z - \epsilon - \Delta_{2\sigma} - \frac{t^2}{z - \epsilon - \Delta_{1\sigma}}}. \end{aligned} \quad (6)$$

The spectral functions are then simply obtained as

$$A_{i\sigma}(\omega) = -\frac{1}{\pi} \text{Im} G_{ii, \sigma}(\omega + i\delta), \quad (7)$$

where $\delta \rightarrow 0^+$.

We now consider the half-metallic limit, $p \rightarrow 1$. For parallel alignment, this implies

$$\Delta_{1\uparrow} = \Delta_{2\uparrow} = \Delta, \quad \Delta_{1\downarrow} = \Delta_{2\downarrow} = 0. \quad (8)$$

We take the wide-band limit where $\Delta = -i\Gamma$. We obtain

$$A_{1\uparrow}(\omega) = A_{2\uparrow}(\omega) = \frac{\Gamma}{\pi} \frac{(\omega - \epsilon)^2 + t^2 + \Gamma^2}{[(\omega - \epsilon + t)^2 + \Gamma^2][(\omega - \epsilon - t)^2 + \Gamma^2]}, \quad (9)$$

and

$$A_{1\downarrow}(\omega) = A_{2\downarrow}(\omega) = \frac{1}{2}\delta(\omega - \epsilon - t) + \frac{1}{2}\delta(\omega - \epsilon + t). \quad (10)$$

For antiparallel alignment we have

$$\Delta_{1\uparrow} = \Delta_{2\downarrow} = \Delta, \quad \Delta_{1\downarrow} = \Delta_{2\uparrow} = 0. \quad (11)$$

It follows

$$A_{1\uparrow}(\omega) = A_{2\downarrow}(\omega) = \frac{\Gamma}{\pi} \frac{(\omega - \epsilon)^2}{t^4 + 2t^2(\omega - \epsilon)^2 + (\omega - \epsilon)^2[\Gamma^2 + (\omega - \epsilon)^2]} \quad (12)$$

and

$$A_{2\uparrow}(\omega) = A_{1\downarrow}(\omega) = \frac{\Gamma}{\pi} \frac{t^2}{t^4 - 2t^2(\omega - \epsilon)^2 + (\omega - \epsilon)^2[\Gamma^2 + (\omega - \epsilon)^2]}. \quad (13)$$

Note that at the particle-hole symmetric point ($\epsilon = 0$), the spectral functions $A_{1\uparrow}$ has a zero while $A_{2\uparrow}$ is finite at $\omega = 0$. This result also holds in the interacting case with $U \neq 0$.